Available online at www.sciencedirect.com
SCIENCE DIRECT®
Polymer 44 (2003) 4443–4454
polymer
www.elsevier.com/locate/polymer

Polyacetylenes bearing mesogenic side groups: synthesis and properties. Part 3. Influence of flexible spacer length and tail functionality

Paola Stagnaro[a], Lucia Conzatti[a], Giovanna Costa[a,*], Bernard Gallot[b], Barbara Valenti[c]

[a]*CNR, Istituto per lo Studio delle Macromolecole ISMAC, Sezione di Genova Via De Marini 6, 16149 Genova, Italy*
[b]*CNRS, Laboratoire des Matériaux Organiques à Propriétées Spécifiques BP 24, 69390 Vernaison, France*
[c]*Università di Genova, Dipartimento di Chimica e Chimica Industriale Via Dodecaneso 31, 16146 Genova, Italy*

Received 21 October 2002; received in revised form 5 May 2003; accepted 15 May 2003

Abstract

We report on the synthesis of some novel liquid crystalline polyacetylenes derived from monosubstituted acetylenic monomers where the acetylenic moiety is linked through a short spacer (one or three methylene units and an ether bridge) to a biphenyl mesogenic core. The influence of length and functionality of the terminal groups on the thermal behaviour and on the nature of the mesophases is discussed. All the monomers show liquid crystalline behaviour. Polymerisations are carried out in solution with typical metathesis catalysts based on Mo and W and yield polyacetylenes with fairly high MW soluble in common organic solvents. Polymers are fully characterised by GPC, FT-IR, and ^{1}H NMR techniques; their thermal and morphological behaviour has been studied by TGA, DSC, POM and X-ray diffraction experiments.

Keywords: Liquid crystalline polyacetylenes; Phase behaviour; X-ray

1. Introduction

Liquid crystalline polymers (LCPs) are of fundamental importance in academic and industrial research: they offer the advantageous combination of the anisotropy of liquid crystals with the attractive bulk properties and processing possibilities of polymers. Among these, LC polyacetylenes have recently drawn a great attention because they are promising candidate materials for opto-electronic applications [1–6]. The introduction of potentially mesogenic substituents, directly linked to a rigid polymer backbone, as the polyene chain, may produce a strong permanent coupling between order and electroactive properties at macroscopic and microscopic level. In fact, the orientation of the side-chains induced by the temperature or by the application of an external electric or magnetic field leads to a LC phase which can induce an anisotropic conformation of the polymer backbone, thus causing an improvement of the main chain conjugation.

A few examples of such polymers are documented in the recent literature [3,4,6–9]; in most cases, they are obtained from monosubstituted acetylenes by using Mo, W or other transition metal based catalysts [4,8–12]. The limited variety of LC polyacetylenes is mainly due to synthetic difficulties related to the design of molecular architectures with the desired LC properties.

Recently, we have investigated the mesomorphic behaviour of several polyacetylenes bearing mesogenic substituents with different chemical structures, linked to the polyene backbone through short flexible spacers [1,2].

In this study, we report on the synthesis and polymerisation of some mesogenic 1-alkynes, abbreviated as **A*n*OBP-R**, bearing a biphenyl moiety as mesogenic core, linked to the acetylenic unit through a short flexible spacer of one or three methylenes and an ether bridge, in order to study the influence of both length and functionality of the tail on the thermal behaviour of the ensuing polymers (**PA*n*OBP-R**).

* Corresponding author. Tel.: +39-010-6475-876; fax: +39-010-6475-880.
E-mail address: costa@ge.ismac.cnr.it (G. Costa).

0032-3861/03/$ - see front matter © 2003 Elsevier Science Ltd. All rights reserved.
doi:10.1016/S0032-3861(03)00414-2

Table 1
Chemical structures of intermediates and monomers **A*n*OBP-R**

A3OBP-R	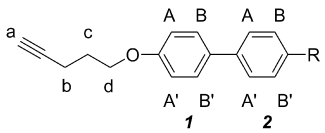
A3OBP-OH	R = –OH
A3OBP-Ac6	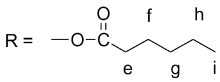
A3OBP-Ac8	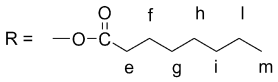
A3OBP-OC8	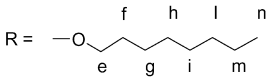
A1OBP-R	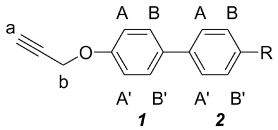
A1OBP-OH	R = –OH
A1OBP-OC8	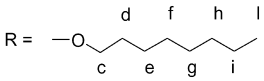

2. Experimental

2.1. Materials

Biphenyl-4,4′-diol (Aldrich, 97%), 3-bromo-1-propyne (Aldrich, 80 wt% in toluene), 5-chloro-1-pentyne (Aldrich, 98%), 1-bromooctane (Fluka, 98 + %), hexanoyl chloride (Fluka, 98 + %), octanoyl chloride (Aldrich, 99%) were all used as received; pyridine (Aldrich, 99 + %) and toluene (Fluka, 99%) were dried and distilled before use; $MoCl_5$ and WCl_6 (Aldrich, 99.9 + %) were used as received; Ph_4Sn (Aldrich, 97%) was recrystallized from $CHCl_3$; catalysts and cocatalyst were stored in a glove box filled with nitrogen at an oxygen content < 5 ppm and moisture content < 1 ppm. Other high-purity solvents and reagents were used as received.

2.2. Characterisation techniques

The ^1H NMR spectra were obtained using a Varian Gemini 200 spectrometer ($CDCl_3$ as solvent and TMS as internal standard). The FT-IR spectra were recorded on a Bruker IFS-28 spectrometer using the KBr method. GPC analysis was carried out with a GPC-SEC Perkin–Elmer chromatograph (Diode Array Detector 235C, eluent THF, flow rate 1ml/min, μ-styragel column set: 10^5,10^4,10^3,500 Å); the calibration curve was obtained with monodispersed polystyrene (PS) standards. A computer-interfaced Mettler DSC 821^e was used for the calorimetric analysis (scanning rate 10 °C/min, under N_2). Optical observations were carried out with a Reichter–Jung Polyvar Pol polarising microscope, equipped with a Mettler FP82HT hot stage connected to a FP80 central processor. A Perkin–Elmer TGA 7 analyser (heating rate 20 °C/min, under N_2) was used to test thermal stabilities. X-ray diffraction experiments were performed on powder samples, with Ni filtrated Cu beam ($\lambda = 1.54$ Å), using a pinhole camera specially designed in the laboratory to operate with powder or oriented samples, under vacuum, and equipped with a device for recording the diffraction patterns of samples at various temperatures between room temperature and 250 °C with an accuracy of 1 °C.

2.3. Synthesis of monomers

The chemical structures of intermediates and monomers are shown in Table 1 The synthetic route is reported in Scheme 1: the alcohol intermediates **AnOBP-OH** were obtained by monoetherification of biphenyl-4,4′-diol with 5-chloro-1-pentyne (for $n = 3$) or 3-bromo-1-propyne (for $n = 1$); monomers **A3OBP-Acn** were synthesized by a

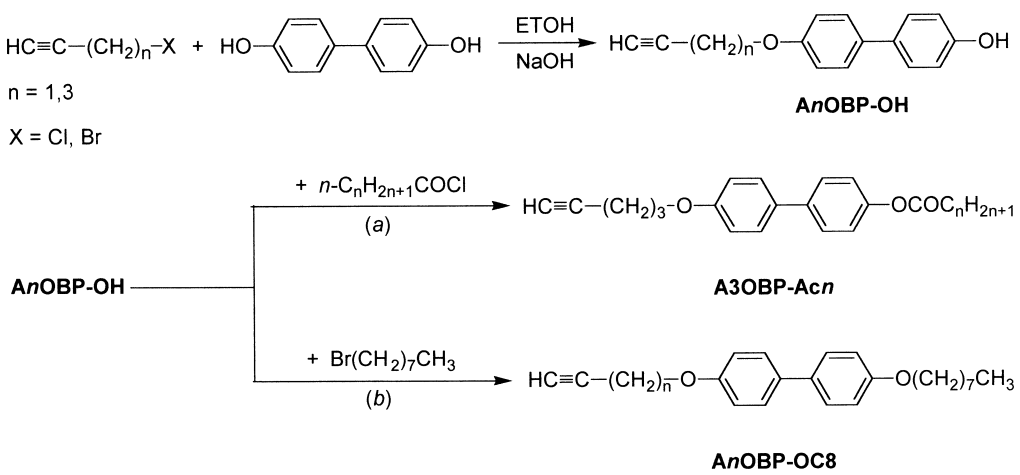

Scheme 1. Synthetic route to monomers A*n*OBP-R.

simple esterification reaction of **A3OBP-OH** with the proper acyl chloride (path a), while monomers **AnOBP-OC8** were prepared by reaction of the alcohol intermediate with 1-bromooctane (path b).

2.3.1. Intermediates

4′-Prop-2-ynyloxy-biphenyl-4-ol **A1OBP-OH**. experimental details on synthesis and characterisation of this intermediate are given in a previous work [2].

4′-Pent-4-ynyloxy-biphenyl-4-ol **A3OBP-OH**. under a dry nitrogen atmosphere, 10 mmol of EtONa (solution 21 wt% in EtOH) first and then 10 mmol of 5-chloro-1-pentyne dissolved in 5 ml of EtOH were added dropwise to a stirred solution of biphenyl-4,4′-diol (10 mmol) and KI (1.2 mmol) in EtOH (12 ml). The reaction mixture was refluxed for 45 h; then, an excess of acidic water was added and EtOH was removed by rotoevaporation. The resultant slurry was extracted with dichloromethane and the organic phase, washed with water and dried over Na_2SO_4, was evaporated under vacuum. The crude product was purified by flash chromatography (eluent: dichloromethane/petroleum ether 1/1 v/v). Beside the desired product, **A3OBP-OH,** a certain amount of 4,4'-bis-pent-4-ynyloxy-biphenyl, **DA3OBP**, given by the etherification of both the OH groups of the substrate, was obtained.

A3OBP-OH. Mp 153 °C; yield 48%. ^{1}H NMR ($CDCl_3$): $\delta = 2.01$ (3H, m, H^a and H^c), 2.43 (2H, td, $J = 2.6$ and 7.0 Hz, H^b), 4.10 (2H, t, $J = 6.0$ Hz, H^d), 6.88 [2H, $(BB')_2$ of $(AA'BB')_2$, $J = 8.4$ Hz], 6.95 [2H, $(AA')_1$ of $(AA'BB')_1$, $J = 8.8$ Hz], 7.43 [2H, $(AA')_2$ of $(AA'BB')_2$, $J = 8.4$ Hz] and 7.45 [2H, $(BB')_1$ of $(AA'BB')_1$, $J = 8.4$ Hz].

IR (KBr): 3359 (m; O–H), 3299 (s; ≡C–H), 2115 (vw; C≡C), 1606 and 1500 (s and vs; arom. ring), 1248 (vs; C–O–C) and 814 cm^{-1}(vs; *p*-subst.).

2.3.2. Esterification reactions

Under a dry nitrogen atmosphere, 7.5 mmol of the proper acyl chloride were added dropwise to an ice cooled solution of **A3OBP-OH** (5 mmol) in 15 ml of anhydrous pyridine. After 20 h stirring at room temperature, the reaction mixture was poured into water and acidified with HCl: the white precipitate was filtered and purified by crystallisation from 2-propanol.

Hexanoic acid 4′-pent-4-ynyloxy-biphenyl-4-yl ester **A3OBP-Ac6**. Mp 119 °C; yield 82%. ^{1}H NMR ($CDCl_3$): $\delta = 0.94$ (3H, t, $J = 6.8$ Hz, H^i), 1.41 (4H, m, H^g and H^h), 1.78 (2H, app quintet, $J = 7.4$ Hz, H^f), 1.98 (1H, t, $J = 2.6$ Hz, H^a), 2.03 (2H, app quintet, $J = 6.5$ Hz, H^c), 2.43 (2H, dt, $J = 2.6$ and 7.0 Hz, H^b), 2.58 (2H, t, $J = 7.5$ Hz, H^e), 4.11 (2H, t, $J = 6.1$ Hz, H^d), 6.97 [2H, $(AA')_1$ of $(AA'BB')_1$, $J = 8.8$ Hz], 7.12 [2H, $(BB')_2$ of $(AA'BB')_2$, $J = 8.7$ Hz], 7.49 [2H, $(BB')_1$ of $(AA'BB')_1$, $J = 8.8$ Hz] and 7.54 [2H, $(AA')_2$ of $(AA'BB')_2$, $J = 8.7$ Hz].

IR (KBr): 3317 (m; ≡C–H), 3042 (w;=C–H), 2956 and 2871 (s; –C–H), 2119 (w; C≡C), 1752 (vs; C=O), 1606 and 1499 (m and s; arom. ring) and 826 cm^{-1} (s; *p*-subst.).

Octanoic acid 4′-pent-4-ynyloxy-biphenyl-4-yl ester **A3OBP-Ac8**. Mp 117 °C; yield 80%. ^{1}H NMR ($CDCl_3$): $\delta = 0.90$ (3H, t, $J = 6.4$ Hz, H^m), 1.38 (8H, m, H^g, H^h, H^i and H^l), 1.77 (2H, app quintet, $J = 7.3$ Hz, H^f), 1.98 (1H, t, $J = 2.6$ Hz, H^a), 2.03 (2H, app quintet, $J = 6.6$ Hz, H^c), 2.43 (2H, dt, $J = 2.6$ and 6.1 Hz, H^b), 2.57 (2H, t, $J = 7.5$ Hz, H^e), 4.11 (2H, t, $J = 6.1$ Hz, H^d), 6.97 [2H, $(AA')_1$ of $(AA'BB')_1$, $J = 8.8$ Hz], 7.12 [2H, $(BB')_2$ of $(AA'BB')_2$, $J = 8.8$ Hz], 7.49 [2H, $(BB')_1$ of $(AA'BB')_1$, $J = 8.8$ Hz] and 7.53 [2H, $(AA')_2$ of $(AA'BB')_2$, $J = 8.8$ Hz].

IR (KBr): 3295 (s; ≡C–H), 3064 (w;=C–H), 2925 and 2853 (vs; –C–H), 2115 (w; C≡C), 1748 (vs; C=O), 1605 and 1498 (s and vs; arom. ring) and 822 cm^{-1} (s; *p*-subst.).

2.3.3. Etherification reactions

The method used is a slight modification of a procedure described in the literature [7]: 2.01 mmol of **A*n*OBP-OH** were added to a solution of KOH (2.8 mmol) in 6.1 ml of EtOH; then 2.21 mmol of 1-bromooctane dissolved in 4.1 ml of EtOH were slowly added into the reaction vessel kept under reflux. After further 5 h refluxing, an excess of water was added. The resultant slurry was extracted with dichloromethane; the organic phase, washed with water and dried over Na_2SO_4, was evaporated under vacuum. The crude product was purified by crystallisation from 2-propanol.

4′-Octyloxy-4-prop-2-ynyloxy-biphenyl **A1OBP-OC8**. Mp 99 °C; yield 47%. ^{1}H NMR ($CDCl_3$): $\delta = 0.89$ (3H, t, $J = 6.6$ Hz, H^l), 1.30 (10H, m, H^e, H^f, H^g, H^h and H^i), 1.80 (2H, app q, $J = 6.6$ Hz, H^d), 2.54 (1H, t, $J = 2.4$ Hz, H^a), 3.98 (2H, t, $J = 6.6$ Hz, H^c), 4.72 (2H, d, $J = 2.2$ Hz, H^b), 6.94 [2H, $(BB')_2$ of $(AA'BB')_2$, $J = 8.8$ Hz], 7.03 [2H, $(AA')_1$ of $(AA'BB')_1$, $J = 9.0$ Hz], 7.46 [2H, $(AA')_2$ of $(AA'BB')_2$, $J = 8.8$ Hz] and 7.49 [2H, $(BB')_1$ of $(AA'BB')_1$, $J = 8.4$ Hz].

IR (KBr): 3285 (m; ≡C–H), 3030 (w;=C–H); 2927 and 2856 (s; –C–H), 2128 (w; C≡C), 1605 and 1499 (s and vs; arom. ring), 1243 (vs; C–O) and 820 cm^{-1} (vs; *p*-subst.).

4′-Octyloxy-4-pent-4-ynyloxy-biphenyl **A3OBP-OC8**. Mp 116 °C; yield 68%. ^{1}H NMR ($CDCl_3$): $\delta = 0.89$ (3H, t, $J = 6.6$ Hz, H^n), 1.31 (10H, m, H^g, H^h, H^i, H^l and H^m), 1.80 (2H, app q, $J = 6.8$ Hz, H^f), 1.98 (1H, app t., $J = 2.8$ Hz, H^a), 2.02 (2H, t, $J = 6.4$ Hz, H^c), 2.43 (2H, dt, $J = 2.6$ and 7.0 Hz, H^b), 3.98 (2H, t, $J = 6.6$ Hz, H^e), 4.10 (2H, t, $J = 6.2$ Hz, H^d), 6.94 [2H, $(BB')_2$ of $(AA'BB')_2$, $J = 8.8$ Hz], 6.95 [2H, $(AA')_1$ of $(AA'BB')_1$, $J = 8.8$ Hz], 7.45 [2H, $(AA')_2$ of $(AA'BB')_2$, $J = 8.8$ Hz] and 7.50 [2H, $(BB')_1$ of $(AA'BB')_1$, $J = 9.1$ Hz].

IR (KBr): 3297 (m; ≡C–H), 3040 (w;=C–H); 2926 and 2855 (s; –C–H), 2116 (w; C≡C), 1606 and 1501 (s and vs; arom. ring), 1248 (vs; C–O) and 824 cm^{-1} (vs; *p*-subst.).

Table 2
Polymerisation of monomer **A3OBP-Ac*n***. Solvent toluene; $[M]_0 = 0.25$ mol/l; $[M]_0/[cat] = 10$; [cat] = [cocat]; reaction time: 21 h; reaction temperature: 80 °C

Run	Monomer	Catalyst	Yield[a] (wt%)	$M_{peak} \times 10^{-3}$[b] (g/mol)
1	**A3OBP-Ac6**	$MoCl_5$	49	6.9
2	**A3OBP-Ac6**	WCl_6	72	11.1
3	**A3OBP-Ac8**	$MoCl_5$	78	7.7
4	**A3OBP-Ac8**	$MoCl_5/Ph_4Sn$	82	9.9
5	**A3OBP-Ac8**	WCl_6	77	10.6
6	**A3OBP-Ac8**	WCl_6/Ph_4Sn	78	6.3

[a] Crude product recovered by precipitation with methanol.
[b] Determined by GPC analysis.

2.4. Polymerisations

Monomers **A*n*OBP-R** were used to prepare several polyacetylenes. Experimental conditions were varied, as reported in Tables 2 and 3. A typical polymerisation procedure is as follows: under a dry nitrogen atmosphere, a weighted amount of catalyst was introduced into a Schlenk reaction vessel together with a portion of the solvent (toluene). If the cocatalyst was used, its solution was prepared in another Schlenk vessel and added to the catalyst solution. The resulting mixture was aged for 15–20 min at 80 °C; then, the required volume of monomer solution was added into the reactor. After 21 h stirring, the polymerisation was stopped by adding a few millilitres of methanol/toluene 1:4 v/v and the quenched mixture was poured into a large excess of methanol.

The precipitate, which was recovered by filtration and dried under vacuum to a constant weight, is generally a mixture of polymer, cyclotrimer and monomer, whose relative amounts depend on the polymerisation conditions. Therefore, pure polymers were isolated by re-dissolving the crude products in THF and adding a measured excess of methanol to precipitate selectively the polymer fraction. In a few cases the cyclic trimer was isolated and characterised; details are given in Section 3.

Table 3
Polymerisation of monomers **AnOBP-OC8**. Solvent toluene; $[M]_0 = 0.25$ mol/l; $[M]_0/[cat] = 10$; [cat] = [cocat]; reaction time: 21 h; reaction temperature: 80 °C

Run	Monomer	Catalyst	Yield[a] (wt%)	$M_{peak} \times 10^{-3}$[b] (g/mol)
1	**A3OBP-OC8**	$MoCl_5$	85	7.9
2	**A3OBP-OC8**	$MoCl_5/Ph_4Sn$	79	10.0
3	**A3OBP-OC8**	WCl_6	89	7.1
4	**A1OBP-OC8**	$MoCl_5$	41[c]	8.9
5	**A1OBP-OC8**	$MoCl_5/Ph_4Sn$	45[c]	9.4
6	**A1OBP-OC8**	WCl_6	60	9.9

[a] Crude product recovered by precipitation with methanol.
[b] Determined by GPC analysis.
[c] The crude product is practically 100% polymer.

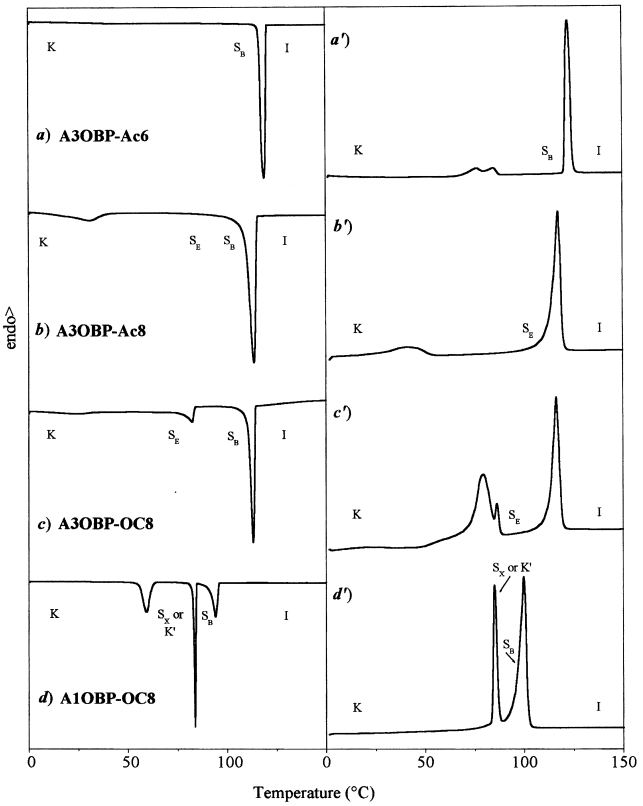

Fig. 1. Cooling and second heating DSC profiles, recorded under nitrogen at a scan rate of 10 °C/min, of monomers: (a), (*a'*) **A3OBP-Ac6**; (b), (*b'*) **A3OBP-Ac8**; (c), (*c'*) **A3OBP-OC8**; (d), (*d'*) **A1OBP-OC8**.

3. Results and discussion

3.1. Monomers

All the monomers are crystalline at room temperature and exhibit liquid crystallinity at higher temperatures, likewise other monosubstituted acetylenes [1,2,4,6,9].

Thermal properties of the monomers are summarised in Table 4. Decomposition temperatures range from 244 to 277 °C; thermotropic behaviour was investigated both by differential scanning calorimetry (DSC) and polarised optical microscopy (POM).

The cooling and the second heating profiles of all the monomers are shown in Fig. 1; DSC traces evidence that crystallisation generally occurs very slowly. POM observations, carried out on cooling the samples starting 20 °C above the clearing point, reveal the formation of smectic textures.

Monomer **A3OBP-Ac6** exhibits two transition peaks in the first heating cycle at 87.5 and 121.3 °C. On cooling, a sharp exotherm at 119.9°C, with only few degrees of undercooling and a very broad transition at lower temperature, hardly detectable in the DSC traces, are present (Fig. 1(a)). With the aid of POM analysis, the first peak on cooling has been assigned to the entrance into a S_B mosaic texture and the broad phenomenon to solidification; since the monomer regenerates this behaviour both on heating and

Table 4
Thermal characterisation of monomers **A*n*OBP-R**

Monomer	T_D[a] (°C)	T_m[b] (°C)	ΔH_m[b] (kcal/mol)	T_i[b] (°C)	ΔH_i[b] (kcal/mol)	T_c[c] (°C)	ΔH_c[c] (kcal/mol)	$T_{i\rightarrow S}$[c] (°C)	$\Delta H_{i\rightarrow S}$[c] (kcal/mol)
A3OBP-Ac6	244	⟨80⟩[d]	0.9	120.6	4.4	⟨45⟩[d]	nd[e]	119.9	4.3
A3OBP-Ac8	277	⟨42⟩[d]	0.8	116.8	4.0	⟨30⟩[d]	0.8	114.5	3.9
A3OBP-OC8	253	⟨83⟩[d]	3.8	116.2	4.5	⟨73⟩[d]	1.6	115.3	4.5
A1OBP-OC8	252	84.2	3.0	99.0	6.5	58.6	3.4	95.1	3.0

[a] Temperature at which the weight loss is 1–2%.
[b] Transition observed during the second DSC heating.
[c] Transition observed during DSC cooling.
[d] Mean value.
[e] Not determined.

on cooling, its thermotropic mesomorphism is enantiotropic. Platelets of the S_B mosaic texture at 119 °C are shown in Fig. 2.

Increasing the tail length with two methylene units (monomer **A3OBP-Ac8**), the DSC traces do not show any significant change, the only difference being a reduced sharpness of the higher temperature signals. POM observations reveal that, upon cooling from the isotropic state, a S_B mosaic texture with lancets appears at 115 °C, as shown in Fig. 3(a). If the temperature is further lowered to 105 °C, striations running across the back of the mosaic appear, which resemble a paramorphotic mosaic texture of a crystal E phase (Fig. 3(b)); this structure persists down to room temperature, since solidification occurs very slowly. On heating colour changes appear around 50 °C and, at about 100 °C, the sample certainly enters the S_E phase; isotropisation occurs at 120 °C.

As to monomer **A3OBP-OC8**, bearing the ether function in the terminal group, the DSC peak at 115.9 °C has been assigned to the transition to a S_B mosaic texture with typical structured lancets, on the base of POM observations on cooling from the isotropic state (Fig. 4(a)); at lower temperatures the presence of striated regions suggest also in this case the occurrence of a $S_B \rightarrow S_E$ transition (Fig. 4(b)). The monomer solidifies at about 80 °C and, in a successive heating run, enters the S_E phase at about 95 °C.

For both monomers, **A3OBP-Ac8** and **A3OBP-OC8**, the second DSC heating run evidences only two transition peaks and no S_B texture is observed on heating, indicating that the S_B mesomorphism could be monotropic or, more probably, enantiotropic over a very narrow range. Variation of the tail functional bridge does not affect the mesomorphic properties of the monomers, whereas reduction of the tail length inhibits the formation of the crystal E phase. Table 4 summarises the thermodynamic parameters associated with the transitions of this series of acetylene monomers; enthalpy variations confirm that the liquid crystal → isotropic transitions are first order in nature and that the mesophases observed should be smectic. However, their high values (close to 4.0–4.5 kcal/mol) could be ascribable to the overlapping of the $S_E \rightarrow S_B$ and $S_B \rightarrow I$ transition, both in the order of 1–2 kcal/mol [13]. The isotropisation temperature and enthalpy appear to be practically unaffected by the nature of the functional bridge and the extension of the alkyl tail. This assumption is confirmed by the results given by Lam et al. [6] for the acetylene monomer which, according to our classification, should be named **A3OBP-Ac12** and shows S_E–S_B mesomorphism.

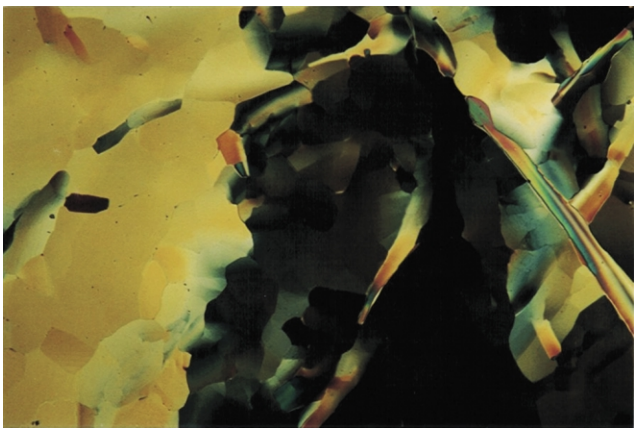

Fig. 2. S_B mosaic texture of monomer **A3OBP-Ac6** at 119 °C.

Monomer **A1OBP-OC8** has a shorter spacer (a single methylene unit) with respect to the previous monomers. Its thermal behaviour presents some differences, as evidenced by the DSC profiles. In the first heating two partially overlapped endothermic peaks are present at about 90 and 100 °C; the same two peaks appear sharper and better resolved in the second heating run (Fig. 1(d)). On cooling, the DSC profile shows three exotherms at 94.8, 85.9 and 59.6 °C (Fig. 1(d)). POM observation, on cooling from the isotropic state, reveals at 98 °C the dendritic growth from the isotropic melt of the mosaic texture of an ordered smectic phase, probably the B phase (Fig. 5(a)); at about 87 °C a further transition (smectic → higher ordered smectic or smectic → crystal transition) takes place, indicated by an evident colour change of the texture (Fig. 5(b)), whereas, around 50 °C clear solidification occurs. On heating, the sample enters the lower temperature smectic or crystal phase at about 85 °C and, probably, the higher temperature mesophase at about 97 °C, very close to the clearing point occurring at 99 °C (Fig. 5(c) could be related to a S_B mosaic texture as a paramorphosis from the solid state).

Fig. 3. POM analysis on monomer **A3OBP-Ac8**: (a) growth of a S_B mosaic texture with lancets and pseudoisotropic regions at 115 °C on cooling; (b) arced mosaic texture at 100 °C.

By comparing monomers **A1OBP-OC8** and **A1OBP-Ac8**, described in our previous paper [2], bearing the same spacer and a tail differently bridged to the rigid core, one can observe that their thermal behaviour is quite different: indeed, monomer **A1OBP-Ac8** shows only a monotropic nematic phase stable in a narrow temperature range (Table 5). Thus, by keeping the same number (8) of carbon atoms and modifying the chemical nature of the tail, from $-OCOC_7H_{15}$ (Ac8) to $-OC_8H_{17}$ (OC8), the LC behaviour of the corresponding monomers changes from monotropic to enantiotropic; moreover, the nature of the mesophase changes from nematic to smectic. In other words, for acetylenes with a very short spacer, only one $-CH_2-$ group, the degree of order increases when the carbonyl group in the tail is replaced by a methylene one.

The overall results summarised in Table 5 indicate that, independently of the flexible spacer, by increasing the tail length melting temperatures and mesophase stability are

Table 5
Mesomorphic properties of monomers **A*n*OBP-R**

Monomer	T_m [a] (°C)	T_i [a] (°C)	LC phase	Monomer[b]	T_m [a] (°C)	T_i [a] (°C)	LC phase
A3OBP-Ac6	⟨80⟩[c]	120.6	S_B	**A1OBP-Ac4**	76.8	–	–
A3OBP-Ac8	⟨42⟩[c]	116.8	K_E-S_B	**A1OBP-Ac6**	53.2	64.4	$S_B-(N)$
A3OBP-Ac12[d]	73.1	116.5	S_E-S_B	**A1OBP-Ac8**	80.6	(65.6)	(N)
A3OBP-OC8	⟨83⟩[c]	116.2	S_E-S_B	**A1OBP-Ac9**	75.5	–	–
A1OBP-OC8	84.2	99	$K(S_?)-S_B$	**A1OBP-Ac10**	⟨79⟩[c]	(72.9)	(N)

[a] Transition observed during the second DSC heating.
[b] From Ref. [2].
[c] Mean value.
[d] From Ref. [6].

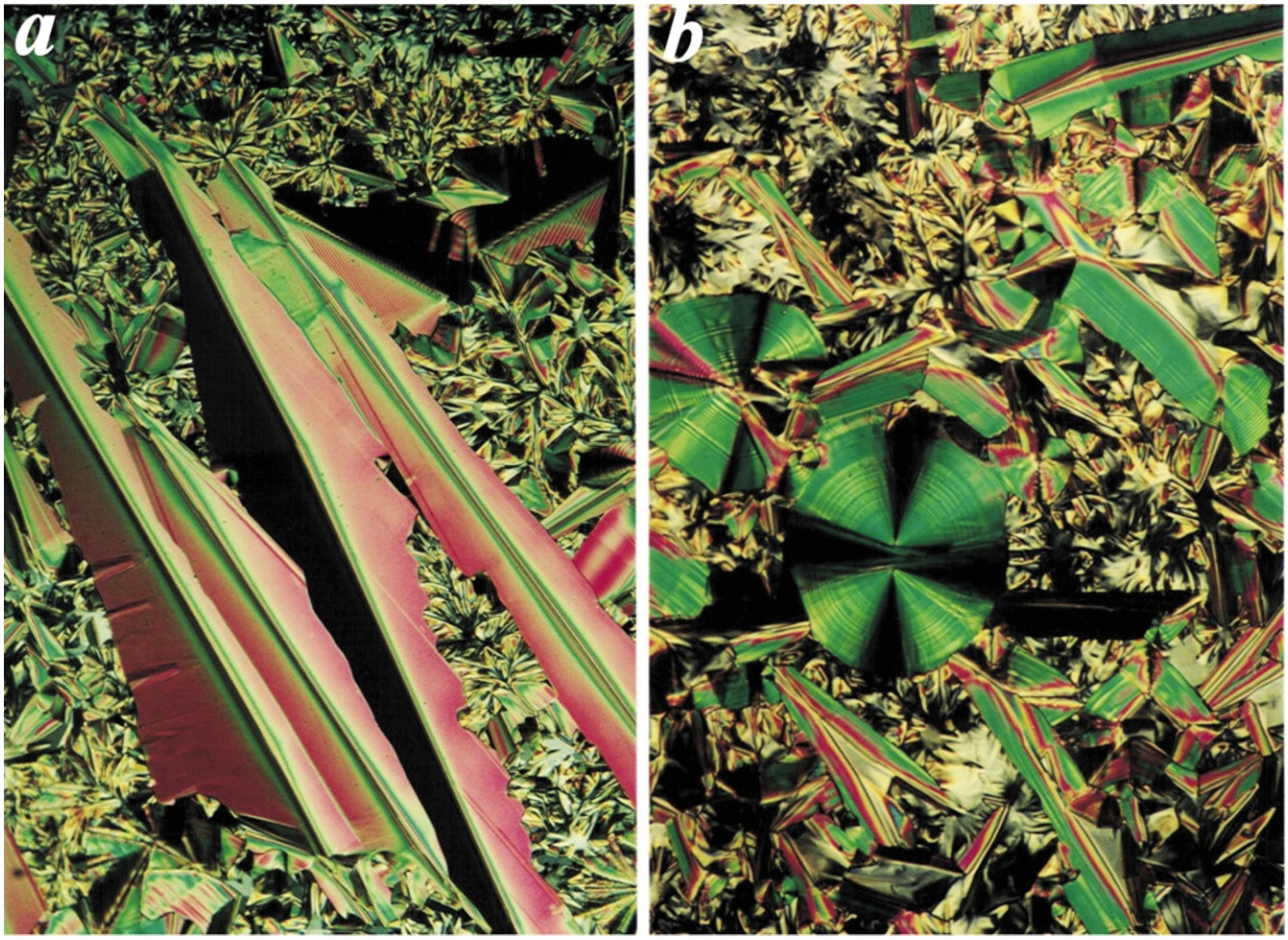

Fig. 4. POM observation on monomer **A3OBP-OC8**: (a) the mosaic texture with typical structured lancets of the S_B phase (112 °C); (b) striated regions at 110 °C.

practically unaffected, apart from monomers **A3OBP-Ac8** and **A1OBP-Ac6**, whose melting temperatures are considerably lower. In both cases the tentative explanation based on the geometrical arrangement in the crystalline phase, given in our previous paper [2], can be invoked: when the side groups attached to the biphenyl core have a slightly different length, as for **A3OBP-Ac8** and **A1OBP-Ac6,** the packing of the molecules in the crystalline phase can be hindered; when the side groups have a similar length (**A3OBP-Ac6** and **A1OBP-Ac4**) or the acyl tail is long enough to give strong interaction between the methylene chains, the crystalline packing is favoured, as indicated by the higher melting temperatures (Table 5).

3.2. Polymers

Several polymerisation runs were carried out with some typical metathesis catalytic systems, based on W and Mo, to study their influence on the reaction products and yields. Both WCl_6 and $MoCl_5$ are effective and the reaction yields, in terms of crude products, are given in Tables 2 and 3. As evidenced by GPC analysis, the polymerisation crude product is generally a mixture of polymer, cyclotrimer and monomer, as already observed [1,2,10,11]; the molecular weights of the high polymer fractions, evaluated on the base of a PS calibration and shown in Tables 2 and 3 as M_{peak} values, depend on the monomer structure and on the specific reaction conditions. The presence of a cocatalyst does not affect the molecular weight and the thermal stability of the resultant polymers; in some cases, it seems to favour the formation of higher amounts of cyclic trimer.

The high polymer has been isolated through a fractional precipitation from THF solutions by adding a proper amount of methanol. Physical properties were determined on purified polymer samples. In a few cases also the cyclic trimer has been isolated and characterised; its structural features indicate the presence of 1,3,5-trisubstituted benzenes, as already observed in previous works [1,2]; this implicates a head-to-tail enchainment fashion of the monomeric units during the polymerisation reaction [14].

All polymers are coloured from orange-red to brownish and soluble in common organic solvents such as THF, toluene, CH_2Cl_2 and $CHCl_3$. Thermal stabilities, obtained

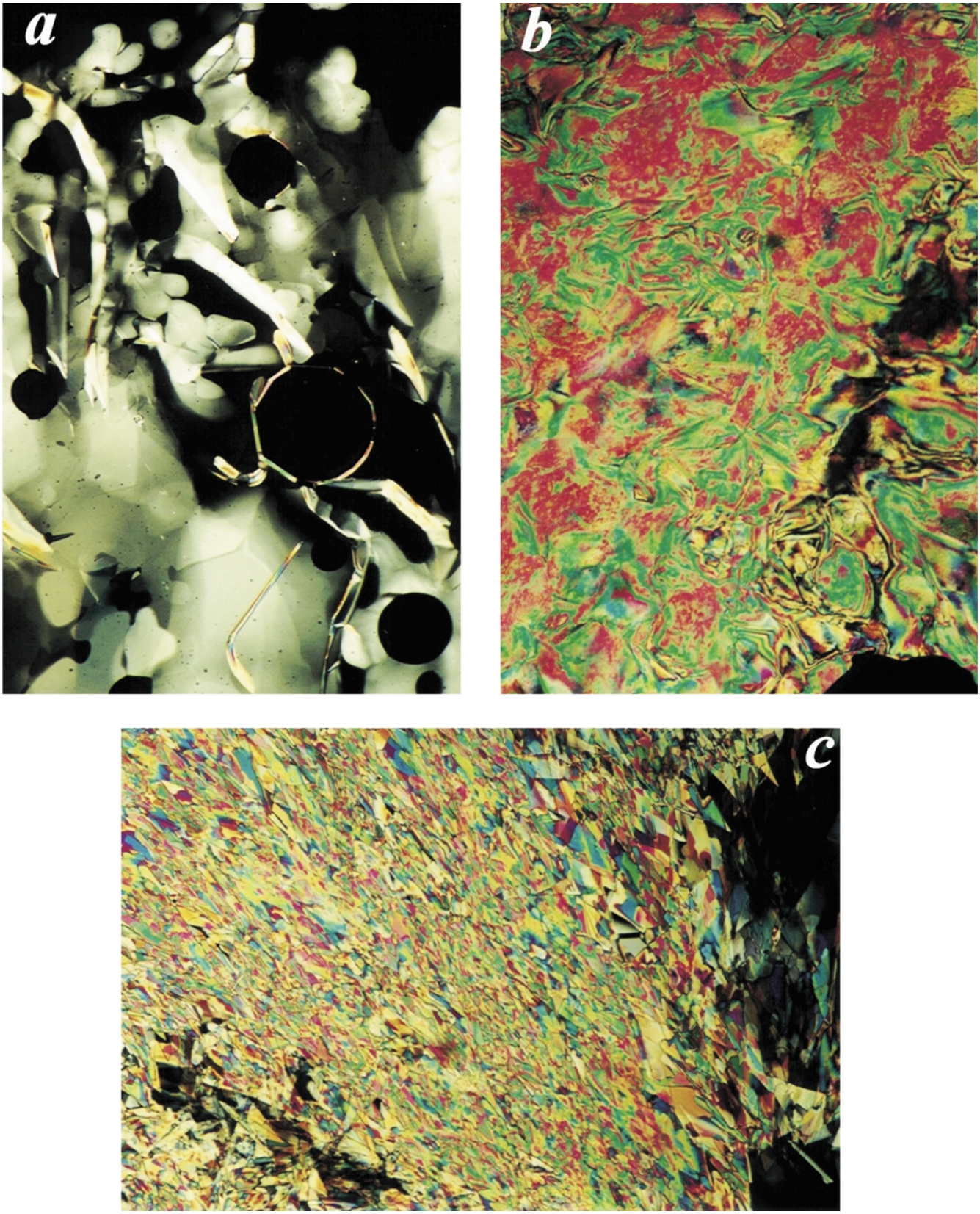

Fig. 5. POM observation on monomer **A1OBP-OC8**: (a) growth from the isotropic melt at 98 °C of the mosaic texture of the S_B phase; (b) smectic → highly order smectic or smectic → crystal transition at about 87 °C; (c) higher temperature mesophase (S_B mosaic texture as a paramorphosis from the solid state) on heating at about 97 °C.

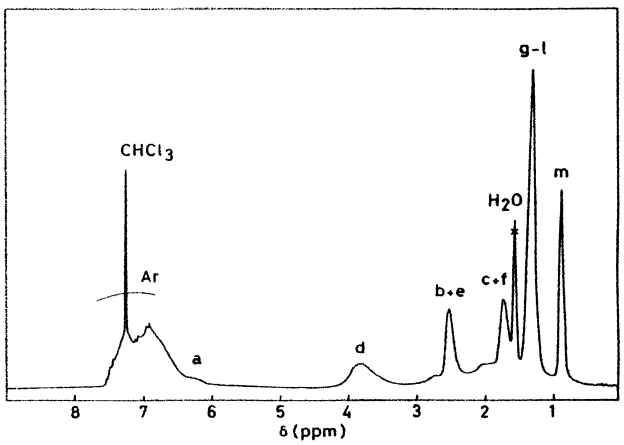

Fig. 6. ^{1}H NMR spectrum ($CDCl_3$, TMS as internal standard) of polymer **PA3OBP-Ac8** (run 5, Table 2).

by TGA analysis under nitrogen atmosphere, are quite high and range from 310 to 350 °C.

The structural characteristics of the resultant polymers have been determined by FT-IR and ^{1}H NMR spectroscopy; in both cases a polyene structure of the backbone has been evidenced. In particular, the absorption bands due to ≡C–H and C≡C stretching vibrations of the monomers are not present anymore in the IR spectra where the frequencies characteristic of the side-chain moieties and of the =C–H stretching vibration in the chain can be observed. In the ^{1}H NMR spectra the proton of the =C–H group of the polyene chain is centred at 6.2 ppm; the broad aspect of this signal suggests a *trans* rich structure of the backbone [1,2,15–17]. An example is given in Fig. 6.

The phase behaviour of the purified samples has been investigated by DSC and POM analyses. For all the polymers a broad exotherm ranging between 90 and 180 °C is present only in the first heating run; as already observed for other polyacetylenes [1,2,4,8,14,15] this peak

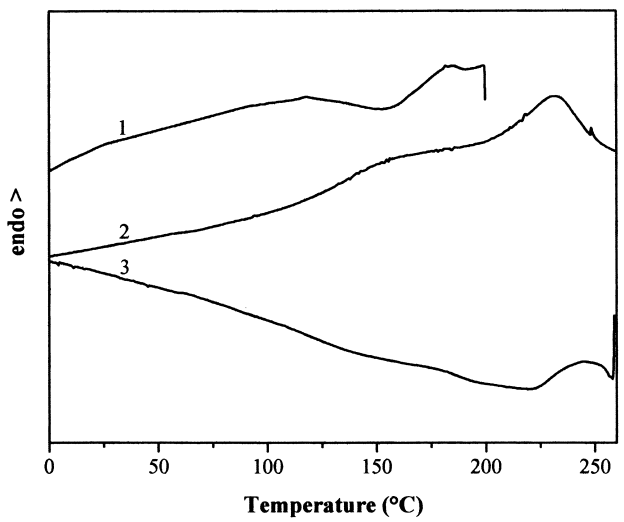

Fig. 7. DSC profiles of **PA3OBP-Ac8** (run 5, Table 2): (1) I heating (2) II heating, (3) II cooling.

can be ascribed to a *cis–trans* isomerisation. The low enthalpy related to this phenomenon (close to 1 kcal/mol) is indicative of a low *cis* double bond content, as confirmed by NMR spectra. At higher temperatures a broad endotherm appears between 190 and 250 °C (related enthalpy in the order of 1 kcal/mol) for polymers bearing the $(CH_2)_3$ spacer, whereas the DSC trace of **PA1OBP-OC8** does not show any other transition besides isomerisation, as already observed for polyacetylenes of the same series [2]. DSC profiles of **PA3OBP-Ac8** are given in Fig. 7. To ascertain the nature of the high temperature transition and to investigate the liquid crystalline behaviour by texture analysis, POM observations have been performed on the purified polymers. The results allow to relate these endotherms to the transition of birefringent specimens to an isotropic liquid, although specific textures cannot be identified on heating; on cooling from the isotropic state the samples enter a smectic phase between 230 and 210 °C. In particular, polymer **PA3OBP-Ac8** (run 5, Table 2) exhibits from about 225 °C the sanded variation of the schlieren texture of the C phase; on cooling to room temperature domain coalescence occurs (Fig. 8(a)) without further significant morphological change. For polymer **PA3OBP-OC8** (run 1, Table 3) the focal-conic texture of the A phase separates from the isotropic liquid at about 220 °C in the form of many small bâtonnets which grow to bigger domains and coalesce when the sample is further cooled (Fig. 8(b)). At lower temperature the texture becomes broken and grained (Fig. 8(c)) and resembles the paramorphotic fans of the C phase; other significant modifications of the texture are not discernible up to room temperature. When polymer **PA3OBP-Ac6** (run 2, Table 2) is cooled from the isotropic state small anisotropic domains emerge at about 220 °C that, on further cooling, resemble the sanded texture of the C phase (Fig. 8(d)). For **PA1OBP-OC8**, POM analysis appears to be not useful due to the poor fluidity and the coloured aspect of the sample, as already observed for similar polymers with one CH_2 spacer [2].

Polymers **PA3OBP-Ac8** (run 5, Table 2), **PA3OBP-OC8** (run 1, Table 3) and **PA1OBP-OC8** (run 5, Table 3) were studied by X-ray diffraction on heating from room temperature up to 200 °C. Independently of the temperature all X-ray diagrams exhibit from one to three sharp reflections in the low angle domain and a band in the wide angle domain (Fig. 9). The low angle reflections can be indexed as the 00 l reflection of a lamellar structure with smectic layers of thickness *d*. The wide-angle signal is characteristic of a disordered smectic structure S_A or S_C [18]. This indicates that the original polymers obtained by precipitation from solution are in a mesomorphic state, as already observed for similar polymers [1,2,8].

The comparison between the thickness *d* of the smectic layers and the length *L* of the repeating unit of the polymers (Table 6), combined with the study of the electron density profiles obtained from the intensities of the low angle reflections [2,19], shows that polymers **PA3OBP-Ac8** and **PA3OBP-OC8**, with a three methylene spacer, exhibit a

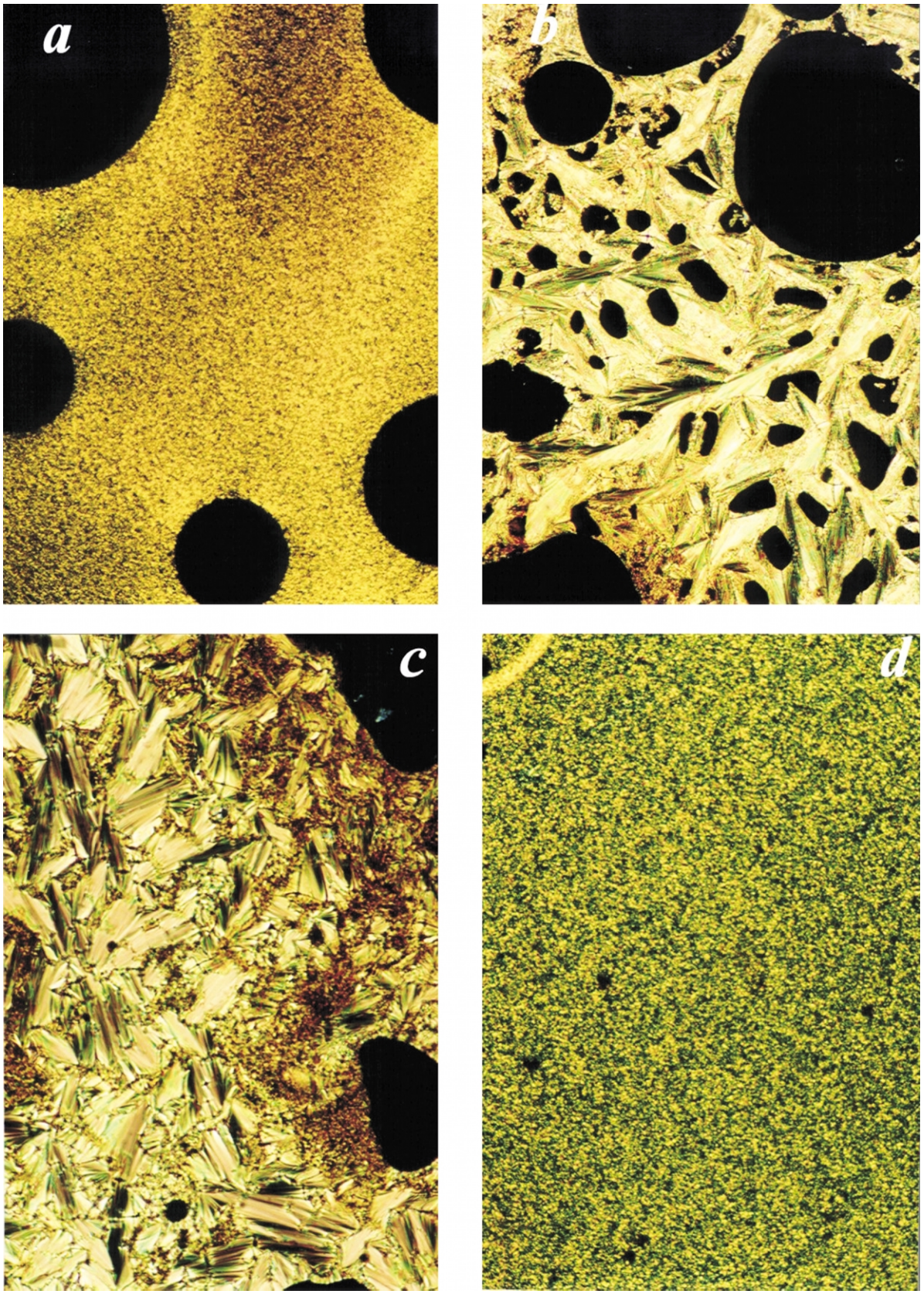

Fig. 8. POM micrographs: (a) the sanded texture of the S_C phase of **PA3OBP-Ac8** at 217 °C; (b) the focal conic fan S_A texture of **PA3OBP-OC8** at 220 °C; (c) the paramorphotic broken focal conic texture of the S_C phase formed on cooling the S_A phase of **PA3OBP-OC8**; (d) the sanded texture of the S_C phase of **PA3OBP-Ac6** at 214 °C.

Table 6
Structural parameters of the mesophase, at room temperature, for polymers **PAnOBP-R**

Polymer	L^a (Å)	$2l + p^b$ (Å)	d^c (Å)	a^d (Å)	α^e (deg.)	Structure
PA1OBP-Ac6	22.1	40.5	37.3	4.6	23	S_{C2}
PA1OBP-Ac8	24.7	45.7	33.9	5.7	0	S_{Ad}
PA1OBP-OC8	24.7	45.7	35.5	5.6	0	S_{Ad}
PA3OBP-OC8	25.2	50.8	46.9	4.6	23	S_{C2}
PA3OBP-Ac8	25.2	50.8	45.2	4.6	27	S_{C2}

[a] Length of the fully extended repeating unit.
[b] l = length of the side chain; p = thickness of the main chain.
[c] Thickness of the smectic layers.
[d] Average distance between side chains.
[e] Tilt angle.

double layer tilted smectic structure S_{C2} (Fig. 10(a)), while polymer **PA1OBP-OC8**, with a single methylene spacer, exhibits a perpendicular interdigitated smectic structure S_{Ad} (Fig. 10(b)). The structural parameters of the three polymers are given in Table 6 together with those related to polymers **PA1OBP-Ac6** and **PA1OBP-Ac8**, studied in our previous work [2].

For the polymers with a single methylene spacer and an eight carbon atom tail, d remains constant upon heating and cooling in the whole temperature range examined whereas, for **PA1OBP-Ac6** with a shorter tail, described in our previous paper [2], the thickness of the smectic layer increases with temperature. For polymers with –Ac8 and –OC8 tails, the reduction of the spacer length from three to one methylene units transforms the double layer tilted smectic S_{C2} structure into a perpendicular interdigitated S_{Ad} structure. Replacing an ether linkage in the tail by an ester one does not change the smectic type S_{C2} or S_{Ad}, at least in the range of temperature investigated by X-ray analysis, but modifies the smectic layer thickness; this involves a change

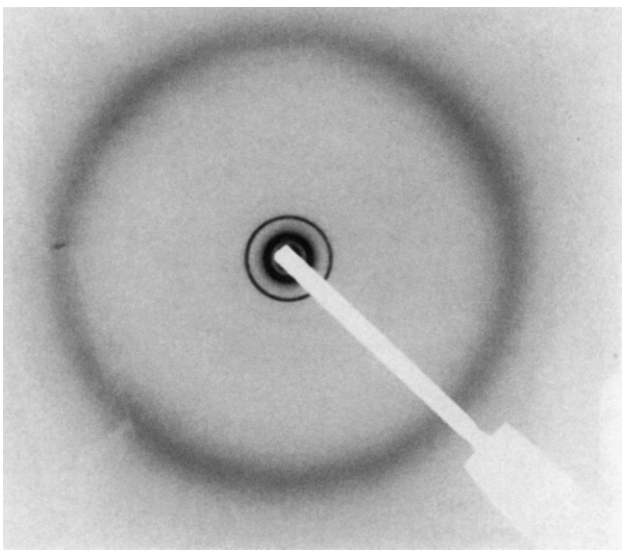

Fig. 9. X-ray diagram of polymer **PA3OBP-OC8** (run 1, Table 3) at room temperature.

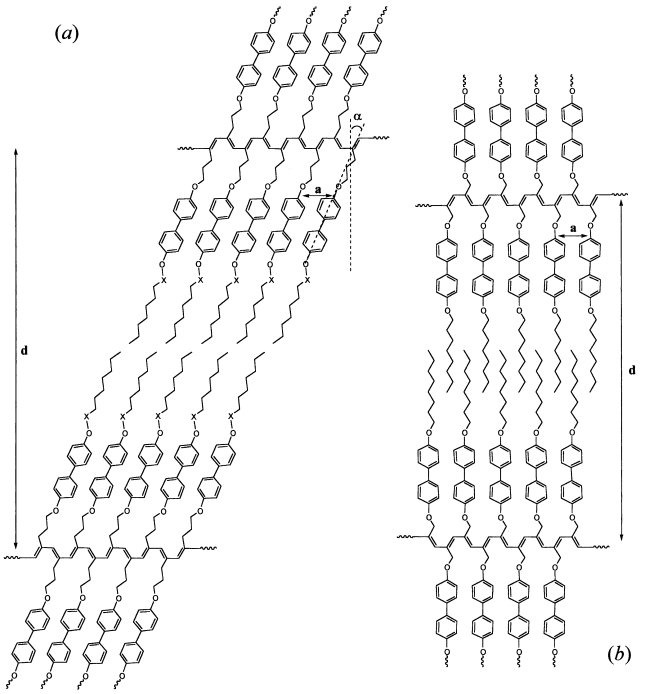

Fig. 10. (a): double layer tilted S_{C2} structures of polymers **PA3OBP-Ac8** (X = CO) and **PA3OBP-OC8** (X = CH_2); (b): double layer interdigitated S_{Ad} structure of polymer **PA1OBP-OC8**.

of the tilt angle in the case of the S_{C2} structure. Indeed, the S_A mesophase for **PA3OBP-OC8** was detected at 220 °C only by POM observations.

4. Conclusive remarks

Novel acetylenic monomers bearing biphenyl mesogenic groups with a short flexible spacer have been synthesised and they all exhibit enantiotropic smectic behaviour. The corresponding polymers are obtained in the ordered phase, directly from the polymerisation reaction. All the polymers studied in this work exhibit smectic structures and the type of mesophase is mainly influenced by the length of the spacer. For polymers with a $(CH_2)_3$ spacer, the predominant phase appears to be the C one; however, by taking into account also literature data related to a polyacetylene with a longer tail [6], which would correspond to **PA3OBP-Ac12**, one can deduce that an increase of the tail length favours the formation of the orthogonal phase, since the mesophase nature goes from S_C for –Ac6 and –Ac8 to S_A for –Ac12. Moreover, the nature of tail linkage (ether instead of ester) induces the formation of a S_A structure which evolves to a S_C at lower temperature.

Acknowledgements

Authors gratefully thank Dr C. Tavani (University of Genova, Italy) for ^{1}H NMR experiments, Mr V. Trefiletti

(ISMAC-CNR Sezione di Genova, Italy) for DSC and TGA measurements and Mr F. Pioli (ISMAC-CNR Sezione di Genova, Italy) for GPC analysis.

References

[1] Stagnaro P, Cavazza B, Trefiletti V, Costa G, Gallot B, Valenti B. Macromol Chem Phys 2001;202:2065. Part 1.
[2] Stagnaro P, Conzatti L, Costa G, Gallot B, Tavani C, Valenti B. Macromol Chem Phys 2003;204:714. Part 2.
[3] Le Moigne J, Hilberer A, Kajazan F. Makromol Chem 1992;193:515.
[4] Akagi K, Shirakawa H. Macromol Symp 1996;104:137.
[5] Huang YM, Lam JWY, Cheuk KKL, Ge W, Tang BZ. Thin Solid Films 2000;363:146.
[6] Lam JWY, Dong Y, Cheuk K.K.L, Luo J, Xie Z, Kwok HS, Mo Z, Tang BZ. Macromolecules 2002;35:1229.
[7] Vicentini F, Mauzac M, Laversanne R, Pochat P, Parneix JP. Liq Cryst 1994;16:721.
[8] Koltzenburg S, Wolff D, Stelzer F, Springer J, Nuyken O. Macromolecules 1998;31:9166.
[9] Lam JWY, Kong X, Dong Y, Cheuk KKL, Xu K, Tang BZ. Macromolecules 2000;33:5027.
[10] Masuda T, Higashimura T. Adv Polym Sci 1987;81:121.
[11] Costa G. Polymerization of mono- and di-substituted acetylenes. In: Eastmond GC, Ledwith A, Russo S, Sigwalt P, editors. Comprehensive polymer science, vol. 4. Oxford: Pergamon Press; 1989. Chapter 9.
[12] Masuda T. In: Chichester J, editor. Catalysis in precision polymerization, 1st ed. New York: Wiley; 1997. Paragraph 2.4.
[13] Gray GW, Goodby JWG. Smectic liquid crystals, 1st ed. Textures and structures, London: L. Hill; 1984.
[14] Kong X, Lam JWY, Tang BZ. Macromolecules 1999;32:1722.
[15] Oh SY, Akagi K, Shirakawa H, Araya K. Macromolecules 1993;26:6203.
[16] Oh SY, Ezaki R, Akagi K, Shirakawa H. J Polym Sci, Part A: Polym Chem 1993;31:2977.
[17] Tang BZ, Kong X, Wan X, Peng H, Lam WY, Feng X-D, Kwok HS. Macromolecules 1998;31:2419.
[18] International tables for X-ray crystallography, Birmingham: Kynoch Press; 1952.
[19] Gudkov A. Sov Phys Crystallography 1984;29:316.